Frontiers of Environmental Science & Engineering
2025, 19(12): 173 https://doi.org/10.1007/s11783-025-2093-5

RESEARCH ARTICLE

Quantifying background $PM_{2.5}$ concentrations in Hainan Province, China through model simulations constrained by multi-source observations

Yibo Zhang[1,2], Yanning Zhang[1,2], Yuhong Guo[3], Jiming Hao[1,2], Wenshuai Xu[4], Weijun Yan[4], Shuxiao Wang[1,2], Qian Song[1,2], Shengyue Li[1,2], Weiling Xiang[5], Li Luo[6], Xiaofeng Huang[7], Zhaohui Yang[8], Xiaochen Wu[8], Yun Zhu[9], Shuhan Liu[6], Bin Zhao ✉ [1,2]

1. State Key Laboratory of Regional Environment and Sustainability, School of Environment, Tsinghua University, Beijing 100084, China
2. State Environmental Protection Key Laboratory of Sources and Control of Air Pollution Complex, Beijing 100084, China
3. College of Tourism and Resources Environment, Zaozhuang University, Zaozhuang 277160, China
4. Hainan Provincial Ecological and Environmental Monitoring Center, Haikou 570206, China
5. State Key Laboratory of Atmospheric Boundary Layer Physics and Atmospheric Chemistry, Institute of Atmospheric Physics, Chinese Academy of Sciences, Beijing 100029, China
6. State Key Laboratory of Marine Resource Utilization in South China Sea, Hainan University, Haikou 570228, China
7. Key Laboratory for Urban Habitat Environmental Science and Technology, School of Environment and Energy, Peking University Shenzhen Graduate School, Shenzhen 518055, China
8. Hainan Research Academy of Environmental Sciences, Haikou 571126, China
9. Guangdong Provincial Key Laboratory of Atmospheric Environment and Pollution Control, College of Environment and Energy, South China University of Technology, Guangzhou Higher Education Mega Center, Guangzhou 510006, China

HIGHLIGHTS

- Local emissions (49.5%) and regional transport (29.3%) dominate Hainan's $PM_{2.5}$.
- Annual mean $PM_{2.5}$ background levels in Hainan are low (4.2–6.9 μg/m^3).
- Estimated $PM_{2.5}$ background values can be decreased by meteorological fluctuations.
- Hainan has high potential to achieve world-leading air quality targets by 2035.

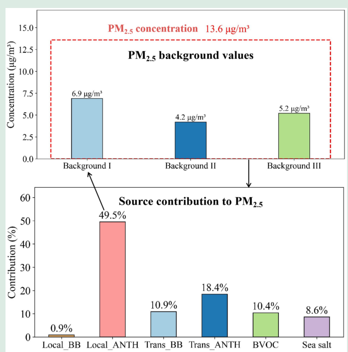

ABSTRACT: As a national ecological civilization pilot zone with unprecedented strategic importance in China, Hainan Province requires precise identification of $PM_{2.5}$ background concentrations to achieve world-leading air quality objectives. This study utilized the three-dimensional regional air quality modeling (WRF-CMAQ) and integrated multi-source ground observation data for model validation. To

✉ Corresponding author. E-mail: bzhao@mail.tsinghua.edu.cn
Article history: Received 25 July 2025, Revised 15 September 2025, Accepted 25 September 2025, Available online 20 October 2025

Special Issue—Atmospheric and Earth System Modeling towards Coordinated Pollution Control and Climate Change Mitigation (Guest Editors: Yuhang Wang, Hongliang Zhang, Yang Gao, Bin Zhao & Peng Wang)

quantify the $PM_{2.5}$ background values for Hainan, representing concentrations largely influenced by natural emissions and regional transport, we determined the contributions from these sources. The results identified local anthropogenic emissions (49.5%) and regional transport (29.3%) as the dominant $PM_{2.5}$ sources in Hainan, with important natural contributions (19.0%). Based on the theoretical definition of background concentrations grounded in scientific research and the objective of providing practical policy insights for Hainan, the $PM_{2.5}$ background values were defined as the $PM_{2.5}$ concentration after (1) excluding local anthropogenic emissions; (2) excluding anthropogenic emissions across Hainan and its surrounding regions; and (3) excluding local emissions combined with projected 2035 emission scenarios for surrounding areas. Based on these three definition methods, the 18 cities-averaged $PM_{2.5}$ background values for Hainan were determined as 6.9, 4.2, and 5.2 μg/m^3, while the corresponding grid-averaged values calculated were 6.7, 4.6, and 4.9 μg/m^3, respectively. Accounting for meteorological fluctuations could yield lower estimated $PM_{2.5}$ concentrations for Hainan. Hainan's $PM_{2.5}$ background values showed comparability with levels documented in clean island areas globally. Our study demonstrated that Hainan maintained a relatively low $PM_{2.5}$ background level, showing substantial emission reduction potential. Through implementation of effective control measures, Hainan is projected to achieve world-leading air quality by 2035.

KEYWORDS: Background value, $PM_{2.5}$ concentration, Source contribution, Hainan Province, CMAQ model

1 Introduction

Hainan Province, China's largest special economic zone, pilot free trade zone, and national ecological civilization pilot zone, has established the most rigorous ecological protection protocols in China through the enforcement of the Hainan Free Trade Port Law. The *Implementation Plan for the National Ecological Civilization Pilot Zone* set forth the objective for Hainan Province to achieve world-leading standards in ecological environment quality and resource utilization efficiency by 2035. Despite Hainan's superior air quality relative to China's mainland, with 2023 annual mean concentrations of SO_2 (3.2 μg/m^3), NO_2 (8.1 μg/m^3), and CO (0.6 mg/m^3) consistently meeting WHO guidelines (WHO, 2021), gaps still existed with the global benchmark. The province's annual $PM_{2.5}$ concentration (12.0 μg/m^3) in 2023 (The People's Government of Hainan Province, 2024) exceeded both the WHO guideline (5 μg/m^3) and the proposed world-class standard of 10 μg/m^3 established by Song et al. (2024) for ecological civilization pilot zones. Moreover, emerging evidence suggested that health risks persist even at low $PM_{2.5}$ concentrations (below 10 μg/m^3), with some studies indicating potentially greater per-unit health impacts at these lower exposure levels (Strak et al., 2021; Weichenthal et al., 2022; Zhao et al., 2024; Zhu et al., 2024) thereby highlighting the critical need for sustained pollution mitigation efforts even in relatively clean regions. Consequently, Hainan Province required advanced control strategies to further reduce $PM_{2.5}$ concentrations.

Under low $PM_{2.5}$ concentration conditions, background values constituted a critical determinant of air quality. The background concentration of $PM_{2.5}$ typically referred to the concentration level unaffected by local emission sources, constituted by natural emissions, such as biogenic volatile organic compounds (BVOCs), biomass burning, sea salt emissions, soil NO_x emissions, soil dust, lightning activity, and contributed by regional transport (Ortiz and Friedrich, 2013; Han et al., 2015; Martín-Cruz et al., 2020). Estimating Hainan's $PM_{2.5}$ background concentration provided a crucial reference for assessing the province's potential for air quality improvement, and constituted a critical foundation for designing effective emission reduction strategies to achieve world-leading air quality goals by 2035. Hainan, situated in the subtropical coastal zone, experienced relatively high natural source emissions including BVOCs and sea salt emissions (Li et al., 2017). Therefore, the background $PM_{2.5}$ concentration in Hainan was significantly influenced by natural sources. Additionally, studies indicated that regional transport contributed substantially to Hainan's $PM_{2.5}$ background concentration (Zhang et al., 2014; Shi et al., 2017; Cao et al., 2023; Xu et al., 2024). Recent assessments employing observation-based source apportionment methods revealed that natural sources accounted for 26% of $PM_{2.5}$ concentration (The People's Government of Hainan Province, 2021). However, conventional observation-based source apportionment methods such as Positive Matrix Factorization (PMF) and Chemical Mass Balance (CMB) face substantial limitations in distinguishing between local and regional transport contributions, and in identifying the contribution of BVOCs (Wang et al., 2018). Although chemical transport models (e.g., CMAQ, WRF-Chem) have demonstrated superior advantages in resolving source-receptor relationships through sensitivity simulations (Tchepel et al., 2010; Guo et al., 2017; Coelho et al., 2023), no study has yet utilized these models to systematically quantify the contributions of natural emissions and regional transport to $PM_{2.5}$ concentrations in Hainan, hindering the determination of its $PM_{2.5}$ background concentration. Furthermore, given that the concept of background concentration can serve different purposes in scientific and policy contexts, adopting distinct definitions of background value for Hainan was necessary and meaningful.

To address these research gaps, this study integrated multiple emission inventories, conducted sensitivity scenario simulations using the CMAQ model, and constrained the modeling results with various observational data (including regular state-controlled stations, background stations, and BVOC measurements), thereby enhancing the reliability of source apportionment. Notably, we propose three distinct definitions of $PM_{2.5}$ background values, each serving different policy-assessment purposes. Furthermore, a future emission scenario was incorporated to evaluate the feasibility of achieving world-leading air quality objectives, providing a forward-looking perspective for policy-making. The research aimed to: (1) assess impacts of natural emissions and regional transport on $PM_{2.5}$ concentrations across Hainan Province; (2) determine the $PM_{2.5}$ background concentration in Hainan and assess the impact of meteorological condition fluctuations on background $PM_{2.5}$ level; (3) compare Hainan's $PM_{2.5}$ background values with those from other clean regions worldwide. The research findings would provide critical scientific support for Hainan's transition toward world-class air quality standards while maintaining its ecological leadership.

2 Materials and methods

2.1 Model configurations

The CMAQv5.3.2 model was employed to investigate contributions of anthropogenic and natural emission sources to $PM_{2.5}$ concentrations in Hainan Province through a nested-domain modeling approach. The modeling framework consisted of two nested domains. The outer domain covered continental China and adjacent Southeast Asian regions with 27 km × 27 km horizontal grid resolution, while the inner domain focused on southern provinces of China, and neighboring Southeast Asian countries including Vietnam, Laos, Myanmar, and Thailand, extending over portions of the South China Sea with higher 9 km × 9 km spatial resolution. Meteorological inputs for the air quality simulations were generated using the Weather Research and Forecasting model version 3.9.1 (WRFv3.9.1). Initial and boundary conditions for the WRFv3.9.1 model were obtained from 1° × 1° Final Global Tropospheric Analysis data (FNL) global analysis dataset provided by the National Centers for Environmental Prediction (NCEP), updated at 6-hour intervals. The four-dimensional data assimilation (FDDA) was applied using the NCEP Automated Data Processing (ADP) Operational Global Surface Observational Data (ds461.0). The WRF configuration incorporated multiple physical parameterizations including the Pleim-Xiu land surface scheme, Asymmetric Convective Model version 2 (ACM2) boundary layer scheme, Grell-Freitas (GF) cumulus parameterization scheme, Rapid Radiative Transfer Model for Global climate models (RRTMG) radiation scheme, and Morrison double-moment cloud microphysics. The outer domain received boundary conditions from global-scale GEOS-Chem simulations, while the inner domain utilized concentration outputs from the parent domain simulations. The CMAQ implementation adopted the SAPRC07 gas-phase chemical mechanism coupled with the AERO07+2D_VBS aerosol module to simulate gas-phase chemistry and aerosol processes. To reduce potential influences from initial conditions, all simulation periods incorporated a 5-d spin-up phase prior to formal analysis periods.

2.2 Emission inventories

The anthropogenic emissions for Hainan emission inventory integrated local air pollutants emissions in Hainan Province and provincial-level air pollutants emissions from the Air Benefit and Cost Attainment Assessment System - Emission Inventory version 2.0 (ABaCAS-EI v2.0) dataset developed by Tsinghua University (Li et al., 2023). The anthropogenic emissions of SO_2, NO_x, and particulate matter (PM) for Hainan were mostly acquired from the Hainan Research

Academy of Environmental Sciences. Specifically, point sources encompassed power plant and industrial process emissions, while non-point sources included on-road vehicle, dust, and commercial cooking emissions. Pollutants emissions from other sectors, VOCs emissions across all sectors in Hainan, and the anthropogenic emissions for China's mainland other than Hainan were adopted from the ABaCAS-EI database (Li et al., 2023). The sector-specific air pollutants emissions in Hainan Province for 2019 were presented in Fig. S1. The foreign anthropogenic emissions were characterized using the Emissions Database for Global Atmospheric Research (EDGAR), jointly released by the Netherlands Environmental Assessment Agency and the European Commission's Joint Research Centre (Crippa et al., 2020). The shipping emissions were obtained from the multi-scale Shipping Emission Inventory Model (SEIM) with a spatial resolution of 0.1 degrees, covering SO_2, NO_x, CO, VOCs, $PM_{2.5}$, OC, and BC (Liu et al., 2016).

Biomass burning emissions were quantified using the Fire Inventory from National Center for Atmospheric Research (NCAR) version 2.5 (FINNv2.5), which calculated gas and particulate emissions from forests and agriculture fires using satellite observations of active fires, land cover, emission factors, and estimated fuel loads (Wiedinmyer et al., 2023). With a high spatiotemporal resolution of 1 km spatially and daily temporally, FINNv2.5 effectively captured the spatio-temporal variations in biomass burning (Wiedinmyer et al., 2023). Biogenic emissions were simulated using MEGANv3.2 (Crippa et al., 2020), and sea salt aerosol emissions were estimated via the CMAQ sea salt module following wind-speed dependent emission schemes (Ovadnevaite et al., 2014). The soil NO_x emissions were calculated online as a function of temperature using MEGANv3.2 (Guenther et al., 2006). The lightning-induced NO_x emissions were estimated using observed lightning flashes along with the assumed NO_x production per flash (Kang et al., 2019).

2.3 Observation data sources

Multiple sources of observational data were used in this study to achieve comprehensive model validation. Hourly $PM_{2.5}$ concentration measurements from 2019 were collected from national control stations in Haikou and Sanya. To enhance the spatiotemporal resolution of validation, daily mean concentrations of inorganic components (e.g., SO_4^{2-}, NO_3^-, CL^-, NH_4^+, K^+, Ca^{2+}, Mg^{2+}, Na^+) for Haikou and Wuzhishan in 2021 were acquired from Hainan University. For regional background validation, this study integrated two complementary observational datasets provided by the Hainan Provincial Environmental Monitoring Center (HPEMC). The first dataset comprised daily average $PM_{2.5}$ concentrations obtaining from the Wuzhishan atmospheric background station (18.81 °N, 109.54 °E), a pristine monitoring site. The second dataset incorporated seasonal $PM_{2.5}$ averages from the Wenchang Puqian Regional Atmospheric Super Station (19.62 °N, 110.89 °E), which had been scientifically established as a representative regional background monitoring facility for Hainan Province. To validate biogenic emission contributions, hourly isoprene concentrations monitored in Sanya (18.25 °N, 109.51°E) during 2019 acquiring from the HPEMC were collected. In addition, radiocarbon (^{14}C) measurements from a coastal background station and an urban station in Shenzhen (Huang et al., 2020; He et al., 2022) were incorporated to quantitatively constrain biogenic contributions.

2.4 Quantification of emission source contributions and background values

The source contributions to $PM_{2.5}$ concentrations in Hainan were quantified using the brute-force method. Based on previous findings demonstrating significant impacts of biomass burning from Southeast Asia on Hainan's air quality (Li et al., 2017; Duc et al., 2021; Qin et al., 2024), we specifically investigated both local and regional biomass burning contributions to $PM_{2.5}$ concentrations in Hainan. Based on preliminary assessments (Murray, 2016; Huang et al., 2023), soil NO_x emissions, lightning NO_x emissions and soil dust were found to contribute minimally to $PM_{2.5}$ in Hainan. Consequently, these sources were included in the emission inputs but were excluded from contribution attribution analysis. The natural sources investigated here comprise biomass burning with wildfire predominance, VOCs emitted from vegetation and sea salt aerosols originating from marine emissions. A series of sensitivity experiments comprising one baseline scenario (Base) and six sensitivity scenarios (Table 1) was established to isolate specific source contributions. The Base scenario incorporated all emission sources, while each sensitivity scenario systematically excluded specific source categories. Differences between the baseline scenario and sensitivity scenarios of No_Local_ANTH, No_Trans_ANTH, No_Local_BB, No_Trans_BB, No_BVOCs, and No_Sea salt respectively represented the contributions of local anthropogenic emissions, regional anthropogenic emissions, local biomass burning, regional biomass burning, BVOCs emissions, and sea

Table 1 Set-up of sensitivity experiments to quantify emission source contributions and $PM_{2.5}$ background values in Hainan

Sensitivity experiments	Configuration of emission sources
Base	Baseline simulations
No_Local_BB	Exclude biomass burning emissions in Hainan
No_Local_ANTH	Exclude anthropogenic emissions in Hainan
No_Trans_BB	Exclude biomass burning emissions in surrounding areas of Hainan
No_Trans_ANTH	Exclude anthropogenic emissions in surrounding areas of Hainan
No_BVOCs	Exclude biogenic VOCs emissions
No_Sea Salt	Exclude sea salt emissions
No_ANTH	Exclude anthropogenic emissions in Hainan and its surrounding regions
No_Local_ANTH_2035	Exclude anthropogenic emissions in Hainan while applying the 2035 anthropogenic emissions under the enhanced control policies (ECP) scenario to the surrounding regions of Hainan

salt emissions to $PM_{2.5}$ in Hainan. The "local emissions" denoted emissions originating within Hainan Province, while "regional emissions" referred to emissions from China's mainland outside Hainan and Southeast Asia within the model domain.

To evaluate seasonal variations in $PM_{2.5}$ concentrations across different emission scenarios, distinct temporal sampling strategies were imple-mented. For the No_Local_ANTH, No_Trans_ANTH, No_BVOCs, and No_Sea salt scenarios, simulations from January, April, July, and October 2019 were selected as seasonal representatives for winter, spring, summer, and autumn, respectively. However, given the substantial monthly variability characteristic of biomass burning emissions relative to other emission sources, we adopted a more comprehensive approach for the Base, No_Local_BB, and No_Trans_BB scenarios to minimize seasonal representation bias. These biomass burning-related scenarios employed full-year 2019 simulations with seasonal classifications as follows: winter (January, February, December), spring (March, April, May), summer (June, July, August), and autumn (September, October, November). This extended sampling framework ensures more robust charac-terization of biomass burning contributions to Hainan's $PM_{2.5}$ concentrations while maintaining temporal comparability across all investigated scenarios.

In the current study, we adopted three definitions to quantify $PM_{2.5}$ background concentrations in Hainan Province, each addressing a specific scientific or policy-management objective. The first definition characterized Hainan's background concentration as $PM_{2.5}$ levels after removing local anthropogenic emissions (labeled as background I). This was a conventional definitions widely adopted in existing studies. The second definition (background II) derived $PM_{2.5}$ background values by excluding anthropogenic emissions from both Hainan and its surrounding regions (all Chinese provinces and Southeast Asian countries within the second model domain that were adjacent to Hainan). This represented a theoretical background level under atmospheric conditions without anthropogenic interference, primarily driven by natural emissions. The third definition quantified Hainan's $PM_{2.5}$ background value by excluding local anthropogenic emissions within Hainan while applying the 2035 anthropogenic emissions under the "enhanced control policies" (ECP) scenario to Hainan's surrounding regions (background III). This ECP scenario assumed smooth implementation of emission reduction measures in China's mainland. It was designed to implement the National Air Quality Continuous Improvement Action Plan, Carbon Peak Implementation Plan, and Beautiful China Initiative. Specifically, the ECP scenario assumed continued future Gross Domestic Product (GDP) growth, albeit at a gradually slowing pace as the economy matures. The energy mix would be significantly optimized, with the share of clean energy installed capacity in the power sector projected to reach 94% by 2035. For the transportation sector, the transition to new energy vehicles would be accelerated, assuming that the share of new energy vehicles in new car sales would gradually approach 100% by 2035. For industrial and other sectors, advanced end-of-pipe control technologies and cleaner production processes would be adopted in the future. This emission scenario forecasted a 35%−65% reduction in anthropogenic emissions in Hainan Province by 2035 compared to the 2019 baseline. Nevertheless, this scenario was subject to uncertainties, primarily including the stringency and timeliness of future policy implementation, the pace of technological advancement and penetration (e.g., in clean energy storage efficiency and pollution control technologies), deviations of actual economic growth from projections. Detailed information regarding the

ECP emission scenario can be found in Song et al. (2024). This prospective definition of background III provided a realistic projection of the background concentration expected by 2035, contingent upon the successful enactment of regional emission reduction policies across mainland China. It directly supported the policy imperative of evaluating the attainability of Hainan's goal to achieve world-leading air quality objectives by 2035. Since publicly reported $PM_{2.5}$ concentrations in Hainan Province were derived from the average of 18 cities monitoring stations, we calculated the background $PM_{2.5}$ concentrations based on model grid averages corresponding to these stations. This station-based approach aligned with China's environmental management protocols, where air quality assessments rely on monitoring station data. By providing background concentrations directly comparable to official reports, our results delivered actionable scientific guidance for Hainan's policymakers. In addition, we also provided $PM_{2.5}$ background values based on the average values across all grids in Hainan Province for comparing with other background value studies. When calculating the $PM_{2.5}$ background values for the 18 cities in Hainan Province, we corrected the simulation results using observational data, following the method of Song et al. (2024). The adjustment was implemented by multiplying the simulated $PM_{2.5}$ concentrations under the scenarios of No_Local_ANTH, No_ANTH, and No_Local_ANTH_2035 by the ratio of BASE scenario simulations to observed concentrations for each city.

2.5 Selection of the most and least favorable meteorological years

Since meteorological conditions could influence background values, we also investigated their impact on $PM_{2.5}$ background values in Hainan. For each month from 2014 to 2023, we identified the four months with the highest and lowest observed $PM_{2.5}$ concentrations in Haikou and Sanya, respectively defined as heavy pollution months and clean months. The average values and anomalies of relative humidity (RH) and northeasterly wind during the heavy pollution months and clean months were calculated for each year from 2014 to 2023. Analysis of annual anomalies in RH and northeasterly wind frequency during heavy pollution months and clean months revealed consistent patterns (Fig. S2). During heavy pollution months, RH exhibited near-universal negative anomalies while northeasterly winds showed predominantly positive anomalies across the years, indicating that low RH and northeasterly winds contribute to pollutant formation or accumulation. For clean months, the relationship with RH anomalies was weaker, but northeasterly winds consistently displayed negative anomalies, demonstrating that southwesterly winds facilitate pollutant dispersion. Based primarily on the annual northeasterly wind anomalies, 2020 was identified as the most meteorologically favorable year for Haikou and Sanya. Conversely, 2019 was determined to be the most meteorologically unfavorable year, as the combined influence of low RH and persistent northeasterly winds directly contributed to the peak $PM_{2.5}$ concentrations observed during its heavy pollution months.

3 Results and discussion

3.1 Model performance

Figure 1(a) presents comparisons of the daily average $PM_{2.5}$ concentrations derived from model simulations and observations at Haikou and Sanya sites. The model demonstrated satisfactory performances for $PM_{2.5}$ across all sites, with normalized mean bias (NMB) values not exceeding ±15.0%. The model accurately captured most $PM_{2.5}$ concentration peaks at Haikou and Sanya sites. The simulated temporal variation of $PM_{2.5}$ concentrations at these sites were in close agreement with the observed data, achieving correlation coefficient (R) values not less than 0.7. We further evaluated the model's performance in simulating inorganic ionic components. Figure 1(b) demonstrates that the model successfully reproduced the concentration levels and seasonal characteristics of inorganic ionic species at both the Haikou and Wuzhishan sites, yielding NMBs of 3.0% and −25.8%, respectively. The model simulated concentrations of inorganic salts (ammonium, nitrate, and sulfate) within reasonable ranges at both locations, with NMBs of 8.4% and 24.2% and RMSEs of 1.1 μg/m^3 and 0.79 μg/m^3 for Haikou and Wuzhishan, respectively. The model captured the observed SO_4^{2-} concentrations well, overestimated NO_3^- at both Haikou and Wuzhishan, and underestimated NH_4^+. For K^+, Ca^{2+}, and Mg^{2+} ions, the simulations generally fell within acceptable bias ranges, showing NMBs of 37.2% and −38.9% and corresponding RMSEs of 0.19 and 0.18 μg/m^3 at Haikou and Wuzhishan, respectively. As the dominant component of sea salt, the accurate simulation of NaCl concentrations served as a critical prerequisite for reliably assessing the model's capability to quantify sea salt contributions to $PM_{2.5}$. As shown in Fig. 1(b), the model successfully reproduced both concentration levels and Seasonal patterns of NaCl, with overall

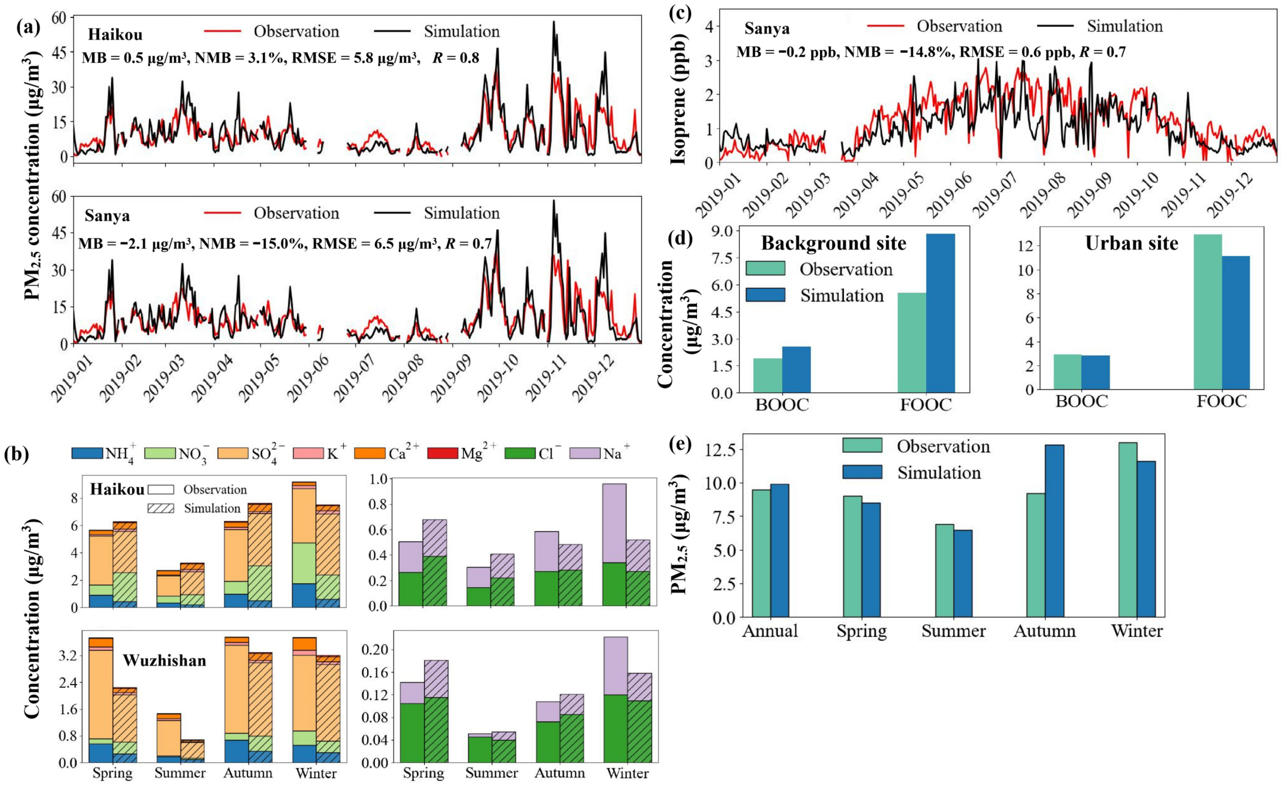

Fig. 1 (a) Comparison of observed and simulated daily $PM_{2.5}$ concentrations at Haikou and Sanya sites; (b) observed and simulated seasonal inorganic components in $PM_{2.5}$ at Haikou and Wuzhishan sites; (c) time series of the observed and simulated daily isoprene concentrations at Sanya site; (d) comparison of observations and simulations of fossil fuel oxygenated organic carbon (FOOC) and biogenic oxygenated organic carbon (BOOC) contributions to OC at background and urban sites in Shenzhen; (e) comparison of observed and simulated annual and seasonal $PM_{2.5}$ concentrations at the Wenchang Puqian background site.

NMBs and RMSEs of −11.2% and 0.25 μg/m^3 for Haikou and −6.6% and 0.11 μg/m^3 for Wuzhishan.

Isoprene, recognized as the predominant BVOCs in terms of global emissions, constituted approximately 50% of total BVOCs emissions (Guenther et al., 2006). A comparison between predicted and observed isoprene concentrations was widely adopted as an effective approach for evaluating the accuracy of biogenic emission inventories (Zhang et al., 2020). Here, we compared the simulated and observed daily mean isoprene concentrations in Sanya, with the results presented in Fig. 1(c). The model reasonably reproduced the isoprene concentrations and their temporal variations in Sanya, exhibiting a NMB of −14.8% and a strong correlation with observations (R = 0.7). This observation constraint enhanced our confidence on the biogenic emission inventory for Hainan used in this study and the model's simulation of BVOCs. Accurate simulation of contributions from natural sources was critical for determining the background $PM_{2.5}$ concentrations in Hainan. Thus, we further constrained the model simulations of BVOCs contributions using observational analytical results of ^{14}C. The ^{14}C content in aerosols served as an effective tracer for distinguishing carbon contributions from non-fossil fuel sources (including BVOCs and biomass burning emissions) and fossil fuel sources. This provided observational evidence to quantify the contributions of BVOCs and biomass burning to organic aerosol (OA). Given that ^{14}C isotopic measurements primarily occurred during non-biomass-burning periods (Huang et al., 2020; He et al., 2022), the identified non-fossil carbon predominantly originated from BVOCs emissions. Comparative analyses were performed at two monitoring sites, the Shenzhen Coastal Background Station representing suburban environments and the Shenzhen Research Academy Site characterizing urban areas. As illustrated in Fig. 1(d), the model simulations revealed BVOCs contributions of 22.5% to organic carbon (OC) at the coastal background station, which was close to the 25.4% estimated through ^{14}C isotopic observations. At the urban site, simulated BVOCs contributions reached 20.3%, showing good agreement with observational estimates of 18.5%. These comparative analyses demonstrated the reliability of the applied methodology in resolving biogenic and anthropogenic influences on aerosol. The simulated isoprene concentrations and BVOCs contributions to OC demonstrated strong consistency with observational data, supporting the reliability of our subsequent quantification of BVOCs contributions to $PM_{2.5}$ in Hainan.

To validate the model's simulation of background $PM_{2.5}$ at the Hainan atmospheric monitoring station, we compared simulated $PM_{2.5}$ concentrations with observational data from Wuzhishan background site and the Wenchang Background Station. The model reproduced the characteristics of $PM_{2.5}$ concentration at Wuzhishan site, with a NMB of 8.0%. At the Wenchang site, the model also demonstrated close agreement with the monitoring site data in both annual averages (with a NMB value of 4.2%) and seasonal variations in Fig. 1(e). This confirmed its reliability in characterizing background concentrations in Hainan.

3.2 Source contributions to $PM_{2.5}$ concentration

Figure 2 illustrates the spatial distribution of annual contributions from six emission sources to annual $PM_{2.5}$ concentrations, while Figure 3 quantifies their seasonal contributions to $PM_{2.5}$ concentrations in Hainan. Local anthropogenic emissions constituted the largest source of $PM_{2.5}$ in Hainan, particularly in northern regions where they contributed over 60% to $PM_{2.5}$ concentrations. The annual average contribution of local anthropogenic emissions to Hainan's $PM_{2.5}$ concentration was 6.75 μg/m^3 (49.5%). Local anthropogenic emissions exhibited pronounced seasonal variability in their contributions to $PM_{2.5}$ concentrations across Hainan Province. Under prevailing southerly winds in summer, regional transport of mainland pollutants subsided substantially, allowing local emissions to dominate $PM_{2.5}$ concentrations in Hainan at 63.9%. While during summer and winter, intensified regional transport decreased local anthropogenic contributions to 39.0%–46.7% of $PM_{2.5}$ concentrations. As shown in Fig. S1, local biomass burning exhibited substantially lower annual emissions of NO_x, SO_2, VOCs, and primary $PM_{2.5}$ (0.5%–4.3%) in Hainan compared to other anthropogenic sources (23.7%–86.9%). Consequently, local biomass burning contributed limited to Hainan's annual $PM_{2.5}$ concentration, averaging 0.12 μg/m^3 (0.9% of total). Seasonal analysis identified spring as the period of maximum influence of local biomass burning on Hainan, accounting for 2.1% of $PM_{2.5}$ concentrations (Fig. 3).

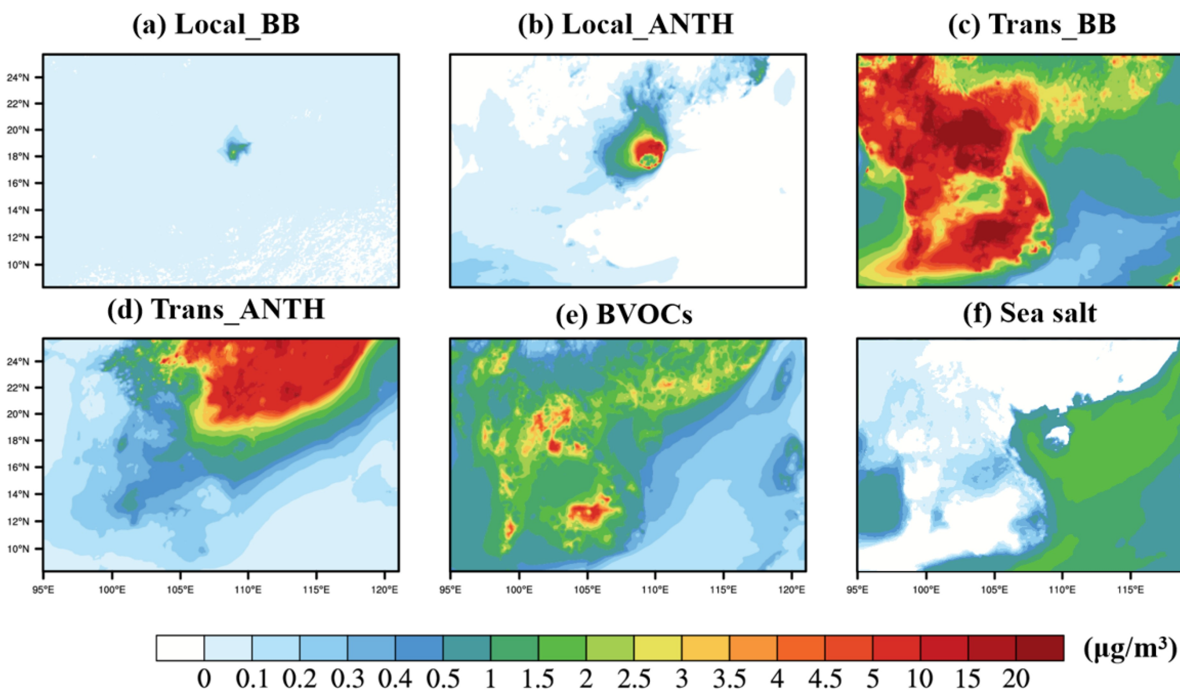

Fig. 2 Spatial distribution of the annual $PM_{2.5}$ contributions from (a) local biomass burning, (b) local anthropogenic emissions, (c)biomass burning in Hainan's surrounding regions, (d) anthropogenic emissions in Hainan's surrounding regions, (e) BVOCs emissions, and (f) sea salt.

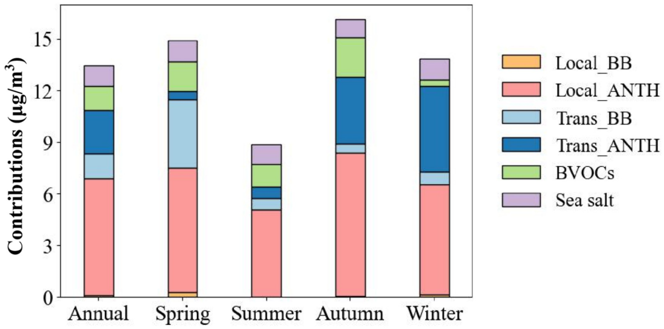

Fig. 3 The annual and seasonal contributions of emission sources to $PM_{2.5}$ concentrations in Hainan.

Anthropogenic emissions from surrounding regions constituted the second-largest $PM_{2.5}$ source in Hainan, just second to local anthropogenic emissions, demonstrating an annual mean concentration of 2.51 μg/m^3 (18.4% of total). The contribution of anthropogenic emissions from surrounding regions exhibited pronounced seasonal variability, with contributions reaching 21.8% in autumn and further intensifying to 30.2% during winter. This seasonal amplification aligned with the northeasterly monsoon patterns, which transported pollutants from the Pearl River Delta region to Hainan during cold seasons. Conversely, the contributions of anthropogenic emissions from surrounding regions were significantly lower in warmer periods, accounting for merely 4.1% and 8.8% of $PM_{2.5}$ concentrations during spring and summer, respectively. Biomass burning constituted a major $PM_{2.5}$ source within Southeast Asian countries, particularly Laos, Myanmar, Thailand, and Vietnam, with the highest annual contribution reaching 58% in Laos. This contribution spatial pattern correlated with the intensity of fire activity mainly caused by forest fires (Le et al., 2020; Yin, 2020; Duc et al., 2021). These high biomass burning emissions in Southeast Asia subsequently influenced Hainan's air quality through regional transport (Yin, 2020; Phuong et al., 2021), contributing 1.48 μg/m^3 (10.9% of total $PM_{2.5}$) annually to $PM_{2.5}$ concentrations in Hainan. Seasonal analysis revealed spring as the peak impact period (31.9%), when enhanced biomass burning in the Southeast Asia regions coincided with westerly transport pathways to Hainan (Zhang et al., 2012). For example, Duc et al. (2021) utilized satellite remote sensing data and the WRF-Chem model, demonstrated that pollutants from biomass burning in Thailand and Laos during spring, 2019 were uplift to high altitude along the Truong Son mountain under westerly wind, and impacted downwind regions including Hainan through long-range transboundary transport. Combined contributions of biomass burning and anthropogenic emissions from Hainan's surrounding regions accounted for 29.3% (3.99 μg/m^3) of the annual mean $PM_{2.5}$ concentrations, highlighting the critical role of regional transport in shaping air quality in Hainan (Zhang et al., 2012, 2014; Zhou et al., 2018). BVOCs emissions contributed 10.4% (1.41 μg/m^3) annually to $PM_{2.5}$ concentration in Hainan, with seasonal peaks reaching 16.5% during summer months due to intensified vegetation metabolic activity. Sea salt emissions predominantly affected coastal zones, contributing 8.6% (1.17 μg/m^3) annually to Hainan's $PM_{2.5}$ concentration, consistent with the source apportionment results of 7% identified by Shi et al. (2017).

3.3 $PM_{2.5}$ background concentration in Hainan

Following the definitions for $PM_{2.5}$ background concentration described in Section 2.4, we determined two types of $PM_{2.5}$ background values for Hainan. One was calculated based on the average concentration across all grids within Hainan and another was derived from the average value of the 18 cities. As illustrated in Fig. 4(a), our analysis showed that the 18 cities-averaged $PM_{2.5}$ background I, II, and III value were 6.9, 4.2, and 5.2 μg/m^3, respectively. The corresponding values derived from the province grid-averaged were 6.7, 4.6, and 4.9 μg/m^3.The annual $PM_{2.5}$ background concentrations obtained using the 18 cities-averaged and the grid-averaged showed minor differences, despite evidently higher observed urban $PM_{2.5}$ concentrations compared to suburban levels across Hainan at present. This occurred because after removing local anthropogenic emissions, the remaining sources exerted a similar influence on $PM_{2.5}$ concentrations across urban, suburban, and rural areas of Hainan. Seasonal analysis demonstrated elevated $PM_{2.5}$ background concentrations during spring, autumn, winter compared to summer. This seasonal variation was associated with the seasonal patterns of biogenic emissions and atmospheric dispersion

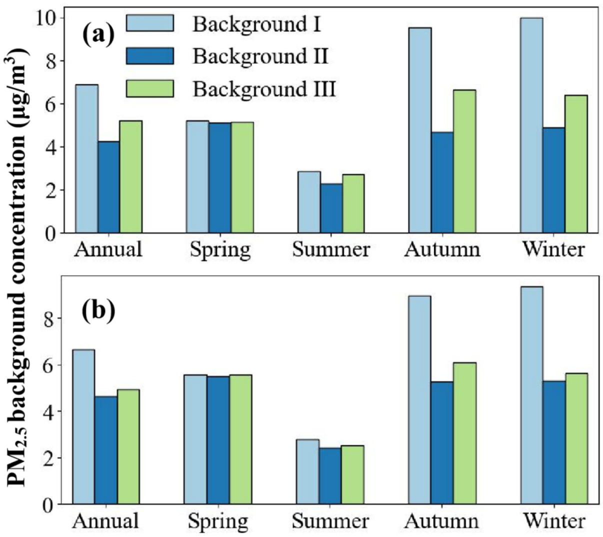

Fig. 4 Annual and seasonal background $PM_{2.5}$ concentrations in Hainan based on the (a) 18 cities-averaged and (b) grid-averaged.

conditions.

Additionally, we compared the current $PM_{2.5}$ concentrations with the background values across 18 cities in Hainan (Fig. S3). After excluding local anthropogenic emissions within Hainan, the background $PM_{2.5}$ concentrations in Hainan ranged from 2.6 to 9.4 μg/m^3. After removing anthropogenic emissions from Hainan and the surrounding regions of Hainan, the background concentrations across the cities ranged between 1.9 and 7.3 μg/m^3. Under the 2035 policy scenario for the surrounding regions combined with the removal of local Hainan anthropogenic emissions, the background values varied from 2.2 to 7.8 μg/m^3. Compared to current levels, the background concentrations calculated using the three definitions decreased by 28.7%–71.8%. Notably, seven cities including Haikou, Sanya, Qionghai, Wanning, Tunchang, Chengmai, and Lingao, showed $PM_{2.5}$ decreases exceeding 50%, demonstrating significant potential for anthropogenic emission reductions in these cities. Overall, Hainan's relatively low $PM_{2.5}$ background levels indicated its considerable remaining potential for anthropogenic emission reductions. Sustained efforts to further decrease $PM_{2.5}$ concentrations could position Hainan to achieve world-leading air quality targets by 2035.

Considering the influence of meteorological conditions on $PM_{2.5}$ background values, we analyzed the $PM_{2.5}$ background values in Hainan under the most favorable and least favorable meteorological years between 2014 and 2023. According to Section 2.5, 2019 served as the baseline simulation year and represented the most meteorologically unfavorable conditions, while 2020 was identified as the most favorable year. It should be noted that the $PM_{2.5}$ background values analyzed here refer to $PM_{2.5}$ concentrations after excluding local anthropogenic emissions in Hainan. The simulation analysis indicated that compared to the 2019 baseline, the favorable meteorological conditions in 2020 resulted in a reduction of 1.6 and 0.8 μg/m^3 in the annual mean $PM_{2.5}$ background value for the grid-averaged and the 18 cities-averaged, respectively (Fig. 5). Seasonally, the favorable meteorological conditions in 2020 resulted in an increase in $PM_{2.5}$ background values during spring, while decreases during summer, autumn, and winter. Overall, accounting for meteorological variability, the $PM_{2.5}$ background levels in other years in Hainan were likely lower than those derived from 2019. This implied greater potential for Hainan to reduce emissions in the future.

3.4 Comparison of $PM_{2.5}$ background concentrations with other clean areas

To understand the level of $PM_{2.5}$ background concentrations in Hainan, we compared Hainan's $PM_{2.5}$ background concentration with previously reported $PM_{2.5}$ background values from other clean regions in China and other countries. The results are presented in Table 2. The $PM_{2.5}$ background values in Table 2 were derived from multiple estimation approaches, including observational sampling methods where background air quality monitoring sites were established in areas with minimal human activity such as mountains and islands, denoted in Table 2 as "Observation". Compared to the $PM_{2.5}$ concentrations measured at atmospheric background stations in China, Hainan's $PM_{2.5}$ background concentration (4.2–6.9 μg/m^3) was significantly lower than values observed at major Chinese atmospheric background stations, including Shenlongjia, Hubei (9.2 μg/m^3; Gao et al., 2020), Menyuan, Qinghai (12.7

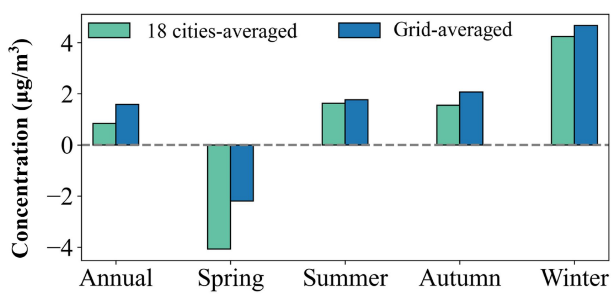

Fig. 5 Changes in background $PM_{2.5}$ values in Hainan due to changes in meteorological conditions in 2020 (favorable year) relative to 2019 (unfavorable year).

Table 2 Summary of domestic and international $PM_{2.5}$ background concentrations in clean areas

ID	Sites	Period	Quantitative methods	Background values	References
1	Shenlongjia, Hubei, China	2017	Observations	9.2	Gao et al., 2020
	Hailuogou, Sichuan, China	2017	Observations	6.7	
	Lijiang, Yunnan, China	2017	Observations	7.6	
	Menyuan, Qinghai, China	2017	Observations	12.7	
	Wuyishan, Fujian, China	2017	Observations	17.3	
2	Changbaishan Mountain, Jilin, China	2012−2014	Observations	17.6±12.6	Liu et al., 2018
	Namtso, Xizang, China	2012−2014	Observations	11.2±6.9	
	Zangdongnan, Xizang, China	2012−2014	Observations	12.3±8.0	
3	Gongga Mountain, Sichuan, China	2017	Observations	6.5 ± 6.2	Cheng et al., 2019
4	Altai, Xinjiang, China	2016	Meteorological filter method	7.8	Wang et al., 2019
5	Taiwan, China	2007	Model simulations	9.0	Chen et al., 2014
6	Taiwan, China	2005−2016	Advanced Global Atmospheric Gas Experiment (AGAGE)	4.4 ± 2.6	Wang et al., 2020
7	London, UK	2009−2010	Model simulations	3.2	Diamantopoulou et al., 2016
	Milan, Italy	2009−2010	Model simulations	5.0	
	Paris, France	2009−2010	Model simulations	4.8	
	Dusseldorf, Germany	2009−2010	Model simulations	5.6	
8	Colorado, USA	2011−2014	Observations	7.9	Stowell et al., 2019
9	Lecce, Italy	2013	Positive Matrix Factorization analysis	6.2	Cesari et al., 2016
10	Europe	1991−2001	Observations	4.8 ± 2.4	Putaud et al., 2004
11	Canary Archipelago	2011−2017	Statistical clustering techniques	4.6 ± 0.4	Cruz et al., 2020
12	Central Israel	2012−2019	Non-negative Matrix Factorization method	4.3 ± 2.5	Belachsen and Broday, 2024
13	Iberian Peninsula	2002−2010	Observations	8.6	Cusack et al., 2012
	Birkenes, Norway	2002−2010	Observations	4.3 ± 1.1	
	Fundao, Portugal	2005−2010	Observations	8.3 ± 1.8	
	Lasmas de Olo, Portugal	2004−2010	Observations	8.3 ± 1.8	
	Campisabalos, Spain	2002−2010	Observations	6.9 ± 0.9	
	Schauinsland, Germany	2002−2009	Observations	7.2 ± 1.7	
	Hyytiala, Finland	2002−2009	Observations	5.5 ± 1.3	
	Aspvreten, Sweden	2002−2010	Observations	7.5 ± 1.3	
14	Aspvreten, Sweden	1997−2010	Observations	8.0	Jönsson et al., 2013

μg/m^3; Gao et al., 2020), Wuyi Mountain (17.3 μg/m^3; Gao et al., 2020), Changbai Mountain (17.6 ± 12.6 μg/m^3; Liu et al., 2018), and Tibetan sites (Namtso: 11.2 ± 6.9 μg/m^3; Zangdongnan: 12.3 ± 8.0 μg/m^3; Liu et al., 2018). It was slightly below Lijiang, Yunnan (7.6 μg/m^3; Gao et al., 2020), and comparable to the $PM_{2.5}$ background levels observed at remote background sites in Sichuan (Hailuogou: 6.7 μg/m^3; Gao et al., 2020; Gongga Mountain: 6.5 ± 6.2 μg/m^3; Cheng et al., 2019). The comparisons indicated that Hainan's $PM_{2.5}$ background value was at a relatively low level compared to other atmospheric background stations in China. It also reflected that, despite most of China's background monitoring sites were situated far from urban areas and lack notable nearby anthropogenic emissions, they were still influenced to some extent by emissions from surrounding regions. Globally, Hainan' s background $PM_{2.5}$ concentrations were comparable to the European background concentrations (Birkenes: 4.3 ± 1.1 μg/m^3; Hyytiälä: 5.5 ± 1.3 μg/m^3; Cusack et al., 2012; regional mean: 4.8 ± 2.4 μg/m^3; Putaud et al., 2004) but remained below North American sites

(Colorado: 7.9 μg/m^3; Stowell et al., 2019; Iberian Peninsula: 8.6 μg/m^3; Cusack et al., 2012). The comparison between urban background sites (e.g., London, Milan, Paris, Düsseldorf) and the Hainan involved inherent differences in spatial representativeness and monitoring conditions. However, it should be noted that this comparison was not intended to equate the two types of sites directly, but rather to provide a broader context for interpreting the $PM_{2.5}$ background levels. Despite differences in site classification, this approach helped to underscore the relatively clean atmospheric background in Hainan compared to other clean regions.

In addition to $PM_{2.5}$ background value comparisons from atmospheric background monitoring sites, we also collected background $PM_{2.5}$ values for global pristine areas derived from various numerical calculation methods. For instance, Hainan's $PM_{2.5}$ background concentrations (4.2–6.9 μg/m^3) were comparable to or slightly higher than values reported for major European cities (Gao et al., 2020) including London (3.2 μg/m^3), Milan (5.0 μg/m^3), Paris (4.8 μg/m^3), and Dusseldorf (5.6 μg/m^3), which were estimated using the three-dimensional PMCAMx transport model coupled with Particulate Matter Source Apportionment Technology (PSAT). The $PM_{2.5}$ background concentrations I (6.7 and 6.9 μg/m^3) estimated for Hainan was comparable to background levels in Italy (6.2 μg/m^3; Cesari et al., 2016) determined through PMF source apportionment. The values were higher than the value reported in Central Israel (4.3 ± 2.5 μg/m^3; Belachsen and Broday, 2024), where background values were determined through factor identification via Non-negative Matrix Factorization method and assessment of air mass source contributions to $PM_{2.5}$. Similarly, the Hainan estimates were higher than the background value obtained for the Canary Archipelago (4.6 ± 0.4 μg/m^3; Martín-Cruz et al., 2020), which was estimated through statistical clustering of the lowest concentration cluster in $PM_{2.5}$ time-series observations. Hainan's $PM_{2.5}$ background level was lower than meteorological-filtered values derived from direct measurements during periods meeting specific lower-layer wind field conditions with no pollution events for Aletai atmospheric background station in Xinjiang (7.8 μg/m^3; Wang et al., 2019). Using a similar local emission zeroing approach through CMAQ model simulation, background concentration I (6.7 and 6.9 μg/m^3) identified for Hainan in this study was markedly lower than the reported background level from Taiwan, China (9.0 μg/m^3; Chen et al., 2014). However, another study applying the Advanced Global Atmospheric Gas Experiment (AGAGE) method, which estimated background concentrations by selecting periods with low $PM_{2.5}$ values, reported a $PM_{2.5}$ background of 4.4 ± 2.6 μg/m^3 for Taiwan, China (Wang et al., 2020). This was lower than Hainan's $PM_{2.5}$ background I (6.7 and 6.9 μg/m^3) and background III (4.9 and 5.2 μg/m^3), whereas it aligned with background concentration II (4.6 and 4.2 μg/m^3). The substantial disparity between two background values from Taiwan was likely attributable to differences in analysis years and methodologies. This underscored the need for caution when comparing $PM_{2.5}$ background levels derived through different research approaches. Overall, despite methodological variations in $PM_{2.5}$ background concentration determination across different studies, comparative analyses with both regional background values using the same CMAQ model simulation approach and atmospheric background station measurements demonstrated Hainan's $PM_{2.5}$ background concentrations at comparable or lower levels.

3.5 Implications for future air quality management

When determining future emission reduction targets, it was necessary to consider background concentrations and their variability influenced by meteorological conditions. It should be noted that the three definitions of $PM_{2.5}$ background values served different purposes. Background I is widely used and directly reflects the current influence of external sources. Background II represented a theoretical lower bound, useful for assessing natural baselines. Background III, which incorporated future emission reductions in surrounding regions, was particularly relevant for policy assessment, as it reflected achievable background levels under realistic regional cooperation scenarios. However, it relied heavily on the accuracy of future emission projections. The selection of an appropriate background definition should align with the spatial scale and policy objective. For city-level management, background I may be more practical as it reflected regional transport influences. For provincial or regional scale, background III offered a forward-looking reference aligned with regional emission policies. If the goal was to assess the maximum potential for air quality improvement, background II provided a theoretical reference under idealized conditions. Our research demonstrated that Hainan's $PM_{2.5}$ background concentrations were generally low using the three definitions. When meteorological variability was considered, these background concentrations may decrease further. Therefore, there was significant potential for further improvement in Hainan's air quality in the future. Continuous implementation of specific control measures targeting energy combustion, industrial processes, transportation sources, and agricultural sources was required to further reduce air pollutants emissions.

In addition, Hainan experienced substantial contributions from anthropogenic emissions transported from surrounding regions, particularly during autumn and winter when $PM_{2.5}$ concentrations were high (Ping et al., 2023). Therefore, reducing the pollution from outside the region was considered crucial for achieving Hainan's air quality goals. It was recommended that Hainan strengthen regional joint prevention and control efforts with other provinces in southeastern China. Specifically, in addressing cross-regional pollution transport, cooperation should be enhanced through mechanisms including information sharing, policy coordination, and joint law enforcement. For instance, under the broader vision of the Beautiful China initiative, Hainan could collaborate with neighboring provinces like Guangdong, Guangxi and Fujian to focus on strengthening $PM_{2.5}$ control measures during winter to mitigate the impact of external pollution on Hainan's air quality. Furthermore, given Hainan's geographical location and the evident impacts from Southeast Asian biomass burning and anthropogenic emissions, exploring the potential of establishing international cooperation mechanisms with neighboring Southeast Asian countries (particularly Vietnam, Laos, and Myanmar) on anthropogenic emission reduction and wildfire prevention was highly recommended.

Driven by Hainan's strategic positioning as a National Ecological Civilization Demonstration Zone requiring world-class air quality, we further assessed the feasibility of achieving the newly proposed world-class ambient air quality standards (AAQS) by 2035 (Song et al., 2024). Adopting the emission scenarios established by Song et al. (2024), we implemented four future emission scenarios based on 2019 emission levels. For Hainan, three scenarios were applied, including "business as usual" (BAU), PC, and "maximum technically feasible reduction" (MTFR) scenarios. For surrounding regions of Hainan in China' s mainland, PC and "conservative" (CONS) scenarios were adopted. We focused on $PM_{2.5}$ concentrations in Hainan when implementing its BAU, PC, and MTFR scenarios while surrounding mainland regions maintained the PC scenario. Additionally, we assessed the compliance of $PM_{2.5}$ concentrations in Hainan under its PC scenario coupled with surrounding regions' CONS scenario, which involves less stringent end-of-pipe control technologies and conservative emission reduction strategies. Using CMAQ sensitivity simulations, we evaluated compliance of annual mean $PM_{2.5}$ concentrations (against 10 μg/m^3) and the annual 95th percentile of daily average $PM_{2.5}$ concentrations (against 20 μg/m^3) across all 18 cities in Hainan under these four scenarios. For a more reasonable assessment of achievability, the projected $PM_{2.5}$ concentrations under future scenarios were corrected using observational data, which was multiplied by the ratio of the simulated value for 2035 to the simulated value for 2019. Simulation results showed that when Hainan and its surrounding regions simultaneously implemented policy control scenarios (PC_PC, PC_MTFR), both the annual mean $PM_{2.5}$ concentrations and the annual 95th percentile of daily $PM_{2.5}$ concentrations met the threshold values in all 18 Hainan cities (Fig. S4). Under the CONS_PC scenario, the annual 95th percentile of daily concentrations still met the threshold across Hainan. Furthermore, the annual mean $PM_{2.5}$ concentrations met the threshold value in all cities except Dongfang. These findings indicated that achieving the world-class air quality standard in Hainan was a realistic prospect. By taking a leading role in China's air quality management efforts, Hainan could provide valuable experiences for air quality improvement in other regions of China and the world.

4 Conclusions

Determining background $PM_{2.5}$ concentration was crucial for setting Hainan's future emission reduction targets and achieving world-leading air quality standards. Hence, this study determined Hainan's background $PM_{2.5}$ concentration in 2019 by quantifying contributions from natural emissions and regional transport using the CMAQ model constrained by observational data. Source apportionment results indicated that natural sources contributed 19.0% to Hainan's annual mean $PM_{2.5}$ concentration. This comprised a 10.4% contribution from BVOCs and 8.6% from marine aerosols. Local anthropogenic emissions (49.5%) and regional transport (29.3%) accounted for the majority of Hainan's annual $PM_{2.5}$ concentration. The regional transport originated predominantly from anthropogenic emissions in surrounding regions (18.4%) and regional biomass burning (10.9%), while local biomass burning made a relatively small contribution (0.9%).

This study employed three definition methods to calculate Hainan's $PM_{2.5}$ background concentration, namely: 1) excluding anthropogenic emissions within Hainan; 2) excluding anthropogenic emissions within both Hainan and its surrounding regions; and 3) application of projected 2035 emission scenarios to the surrounding regions while excluding anthropogenic emissions within Hainan. Under these three definitions, the estimated annual mean $PM_{2.5}$ background values averaged across the 18 cities in Hainan were 6.9, 4.2, and 5.2 μg/m^3, respectively. Correspondingly, the grid-averaged $PM_{2.5}$ background values for Hainan were 6.7, 4.6, and 4.9 μg/m^3, respectively. Meteorological variability analysis revealed further decrease in Hainan's $PM_{2.5}$ background concentration under 2020's favorable meteorological conditions compared to 2019's unfavorable conditions used above. Compared to background levels in other island regions globally, Hainan's $PM_{2.5}$ background concentration was found to be comparable.

Hainan's $PM_{2.5}$ background concentration was maintained at a low level, indicating significant potential for further air quality improvement. When both Hainan and its surrounding regions employed the policy scenario, the model demonstrated that the annual average $PM_{2.5}$ concentration and the annual 95th percentile of daily average $PM_{2.5}$ concentrations across all 18 cities in Hainan could meet the newly proposed AAQS standards. This finding indicated that achieving world-leading air quality levels in Hainan by 2035 was prospective.

Conflict of Interests Jiming Hao is the Advisory Board member of F*rontiers of Environmental Science & Engineering*. The authors declare that the research was conducted in the absence of any commercial or financial relationships that could be construed as a potential conflict of interest.

Acknowledgements This work was supported by the National Key R&D Program of China (No. 2022YFC3700702), the specific research fund of The Innovation Platform for Academicians of Hainan Province (No. YSPTZX202512), the National Natural Science Foundation of China (No. 42307130), the China Postdoctoral Science Foundation (No. 2023M741936).

Electronic Supplementary Material Supplementary material is available in the online version of this article at https://doi.org/10.1007/s11783-025-2093-5 and is accessible for authorized users.

References

Belachsen I, Broday D M (2024). Decomposing $PM_{2.5}$ concentrations in urban environments into meaningful factors: 1. Separating the contribution of local anthropogenic activities from background and long-range transport. Science of the Total Environment, 940: 173749

Cao X C, Xing Q, Hu S H, Xu W S, Xie R F, Xian A D, Xie W J, Yang Z H, Wu X C (2023). Characterization, reactivity, source apportionment, and potential source areas of ambient volatile organic compounds in a typical tropical city. Journal of Environmental Sciences, 123: 417–429

Cesari D, Donateo A, Conte M, Merico E, Giangreco A, Giangreco F, Contini D (2016). An inter-comparison of $PM_{2.5}$ at urban and urban background sites: chemical characterization and source apportionment. Atmospheric Research, 174–175: 106–119

Chen T F, Chang K H, Tsai C Y (2014). Modeling direct and indirect effect of long range transport on atmospheric $PM_{2.5}$ levels. Atmospheric Environment, 89: 1–9

Cheng L J, Ji D S, He J, Li L, Du L, Cui Y, Zhang H L, Zhou L X, Li Z Q, Zhou Y X, et al. (2019). Characteristics of air pollutants and greenhouse gases at a regional background station in Southwestern China. Aerosol and Air Quality Research, 19(5): 1007–1023

Coelho S, Ferreira J, Lopes M (2023). Source apportionment of air pollution in urban areas: a review of the most suitable source-oriented models. Air Quality, Atmosphere & Health, 16(6): 1185–1194

Crippa M, Solazzo E, Huang G L, Guizzardi D, Koffi E, Muntean M, Schieberle C, Friedrich R, Janssens-Maenhout G (2020). High resolution temporal profiles in the emissions database for global atmospheric research. Scientific Data, 7(1): 121

Cusack M, Alastuey A, Pérez N, Pey J, Querol X (2012). Trends of particulate matter ($PM_{2.5}$) and chemical composition at a regional background site in the western Mediterranean over the last nine years (2002–2010). Atmospheric Chemistry and Physics, 12(18): 8341–8357

Diamantopoulou M, Skyllakou K, Pandis S N (2016). Estimation of the local and long-range contributions to particulate matter levels using continuous measurements in a single urban background site. Atmospheric Environment, 134: 1–9

Duc H N, Bang H Q, Quan N H, Quang N X (2021). Impact of biomass burnings in southeast Asia on air quality and pollutant transport during the end of the 2019 dry season. Environmental Monitoring and Assessment, 193(9): 565

Gao L, Yue X, Meng X Y, Du L, Lei Y D, Tian C G, Qiu L (2020). Comparison of ozone and $PM_{2.5}$ concentrations over urban, suburban, and background sites in China. Advances in Atmospheric Sciences, 37(12): 1297–1309

Guenther A, Karl T, Harley P, Wiedinmyer C, Palmer P I, Geron C (2006). Estimates of global terrestrial isoprene emissions using MEGAN (Model of Emissions of Gases and Aerosols from

Nature). Atmospheric Chemistry and Physics, 6(11): 3181–3210

Guo H, Kota S H, Sahu S K, Hu J L, Ying Q, Gao A F, Zhang H L (2017). Source apportionment of $PM_{2.5}$ in North India using source-oriented air quality models. Environmental Pollution, 231: 426–436

Han S, Zhang Y, Wu J, Zhang X, Tian Y, Wang Y, Ding J, Yan W, Bi X, Shi G, et al. (2015). Evaluation of regional background particulate matter concentration based on vertical distribution characteristics. Atmospheric Chemistry and Physics, 15(19): 11165–11177

He D Y, Huang X F, Wei J, Wei F H, Zhu B, Cao L M, He L Y (2022). Soil dust as a potential bridge from biogenic volatile organic compounds to secondary organic aerosol in a rural environment. Environmental Pollution, 298: 118840

Huang L, Fang J, Liao J Q, Yarwood G, Chen H, Wang Y J, Li L (2023). Insights into soil NO emissions and the contribution to surface ozone formation in China. Atmospheric Chemistry and Physics, 23(23): 14919–14932

Huang X F, Dai J, Zhu Q, Yu K Y, Du K (2020). Abundant biogenic oxygenated organic aerosol in atmospheric coarse particles: plausible sources and atmospheric implications. Environmental Science & Technology, 54(3): 1425–1430

Jönsson O, Andersson C, Forsberg B, Johansson C (2013). Air pollution episodes in Stockholm regional background air due to sources in Europe and their effects on human population. Boreal Environment Research, 18(3−4): 280–302

Kang D W, Foley K M, Mathur R, Roselle S J, Pickering K E, Allen D J (2019). Simulating lightning NO production in CMAQv5.2: performance evaluations. Geoscientific Model Development, 12(10): 4409–4424

Le H A, Phuong D M, Linh L T (2020). Emission inventories of rice straw open burning in the Red River Delta of Vietnam: evaluation of the potential of satellite data. Environmental Pollution, 260: 113972

Li J, Zhang Y Q, Wang Z F, Sun Y L, Fu P Q, Yang Y C, Huang H L, Li J J, Zhang Q, Lin C Y, et al. (2017). Regional impact of biomass burning in southeast Asia on atmospheric aerosols during the 2013 seven South-East Asian studies project. Aerosol and Air Quality Research, 17(12): 2924–2941

Li S Y, Wang S X, Wu Q R, Zhang Y N, Ouyang D W, Zheng H T, Han L C, Qiu X H, Wen Y F, Liu M, et al. (2023). Emission trends of air pollutants and CO_2 in China from 2005 to 2021. Earth System Science Data, 15(6): 2279–2294

Liu H, Fu M L, Jin X X, Shang Y, Shindell D, Faluvegi G, Shindell C, He K B (2016). Health and climate impacts of ocean-going vessels in east Asia. Nature Climate Change, 6(11): 1037–1041

Liu Z R, Gao W K, Yu Y C, Hu B, Xin J Y, Sun Y, Wang L L, Wang G H, Bi X H, Zhang G H, et al. (2018). Characteristics of $PM_{2.5}$ mass concentrations and chemical species in urban and background areas of China: emerging results from the CARE-China network. Atmospheric Chemistry and Physics, 18(12): 8849–8871

Martín-Cruz Y, Vera-Castellano A, Gómez-Losada Á (2020). Characterization of background particulate matter concentrations using the combination of two clustering techniques in zones with heterogeneous emission sources. Atmospheric Environment, 243: 117832

Murray L T (2016). Lightning NO_x and impacts on air quality. Current Pollution Reports, 2(2): 115–133

Ortiz S T, Friedrich R (2013). A modelling approach for estimating background pollutant concentrations in urban areas. Atmospheric Pollution Research, 4(2): 147–156

Ovadnevaite J, Manders A, De Leeuw G, Ceburnis D, Monahan C, Partanen A I, Korhonen H, O'dowd C D (2014). A sea spray aerosol flux parameterization encapsulating wave state. Atmospheric Chemistry and Physics, 14(4): 1837–1852

Phuong P T H, Nghiem T D, Thao P T M, Pham C T, Thi T T, Dien N T (2021). Impact of rice straw open burning on local air quality in the Mekong Delta of Vietnam. Atmospheric Pollution Research, 12(11): 101225

Ping L Y, Wang Y, Lu Y L, Lee L C, Liang C (2023). Tracing the sources of $PM_{2.5}$-related health burden in China. Environmental Pollution, 327: 121544

Putaud J P, Raes F, Van Dingenen R, Brüggemann E, Facchini M C, Decesari S, Fuzzi S, Gehrig R, Hüglin C, Laj P, et al. (2004). A European aerosol phenomenology—2: chemical characteristics of particulate matter at kerbside, urban, rural and background sites in Europe. Atmospheric Environment, 38(16): 2579–2595

Qin Y J, Wang H C, Wang Y M, Lu X, Tang H R, Zhang J Q, Li L, Fan S J (2024). Wildfires in southeast Asia pollute the atmosphere in the northern South China Sea. Science Bulletin, 69(8): 1011–1015

Shi Z H, Li J Y, Huang L, Wang P, Wu L, Ying Q, Zhang H L, Lu L, Liu X J, Liao H, et al. (2017). Source apportionment of fine particulate matter in China in 2013 using a source-oriented chemical transport model. Science of the Total Environment, 601–602: 1476–1487

Song Q, Zhang N N, Zhang Y N, Yin D J, Hao J M, Wang S X, Li S Y, Xu W S, Yan W J, Meng X X, et al. (2024). The development of local ambient air quality standards: a case study of Hainan Province, China. Eco-Environment & Health, 3(1): 11–20

Stowell J D, Geng G N, Saikawa E, Chang H H, Fu J S, Yang C E, Zhu Q Z, Liu Y, Strickland M J (2019). Associations of wildfire smoke $PM_{2.5}$ exposure with cardiorespiratory events in Colorado 2011–2014. Environment International, 133: 105151

Strak M, Weinmayr G, Rodopoulou S, Chen J, de Hoogh K, Andersen Z J, Atkinson R, Bauwelinck M, Bekkevold T, Bellander T, et al. (2021). Long term exposure to low level air pollution and mortality in eight European cohorts within the ELAPSE project: pooled analysis. BMJ, 374: n1904

Tchepel O, Costa A M, Martins H, Ferreira J, Monteiro A, Miranda A I, Borrego C (2010). Determination of background concentrations for air quality models using spectral analysis and filtering of monitoring data. Atmospheric Environment, 44(1): 106–114

The People’s Government of Hainan Province (2021). Bulletin on the State of Ecology and Environment of Hainan Province 2020.

Zhengzhou: The People's Government of Hainan Province

The People's Government of Hainan Province (2024). Bulletin on the State of Ecology and Environment of Hainan Province 2023. Zhengzhou: The People's Government of Hainan Province

Wang P, Ying Q, Zhang H L, Hu J L, Lin Y C, Mao H J (2018). Source apportionment of secondary organic aerosol in China using a regional source-oriented chemical transport model and two emission inventories. Environmental Pollution, 237: 756–766

Wang S H, Hung R Y, Lin N H, Gómez-Losada A, Pires J C M, Shimada K, Hatakeyama S, Takami A (2020). Estimation of background $PM_{2.5}$ concentrations for an air-polluted environment. Atmospheric Research, 231: 104636

Wang Y Q, Zhang J Q, Bai Z P, Yang W, Zhang H, Mao J, Sun Y L, Ma Z X, Xiao J, Gao S, et al. (2019). Background concentrations of PMs in Xinjiang, West China: an estimation based on meteorological filter method and Eckhardt algorithm. Atmospheric Research, 215: 141–148

Weichenthal S, Pinault L, Christidis T, Burnett R T, Brook J R, Chu Y, Crouse D L, Erickson A C, Hystad P, Li C, et al. (2022). How low can you go? Air pollution affects mortality at very low levels. Science Advances, 8(39): eabo3381

Wiedinmyer C, Kimura Y, McDonald-Buller E C, Emmons L K, Buchholz R R, Tang W F, Seto K, Joseph M B, Barsanti K C, Carlton A G, et al. (2023). The fire inventory from NCAR version 2.5: an updated global fire emissions model for climate and chemistry applications. Geoscientific Model Development, 16(13): 3873–3891

WHO (2021). WHO Global Air Quality Guidelines: Particulate Matter ($PM_{2.5}$ and PM_{10}), Ozone, Nitrogen Dioxide, Sulfur Dioxide and Carbon Monoxide. Geneva: World Health Organization

Xu W S, Xing Q, Pan L B, Wang Z S, Cao X C, Yan W J, Xie W J, Meng X X, Wu X C (2024). Characterization, source apportionment, and risk assessment of ambient volatile organic compounds in urban and background regions of Hainan Island, China. Atmospheric Environment, 316: 120167

Yin S (2020). Biomass burning spatiotemporal variations over south and southeast Asia. Environment International, 145: 106153

Zhang Y L, Li J, Zhang G, Zotter P, Huang R J, Tang J H, Wacker L, Prévôt A S H, Szidat S (2014). Radiocarbon-based source apportionment of carbonaceous aerosols at a regional background site on Hainan Island, South China. Environmental Science & Technology, 48(5): 2651–2659

Zhang Y L, Zhang R X, Yu J Z, Zhang Z, Yang W Q, Zhang H N, Lyu S J, Wang Y S, Dai W, Wang Y H, Wang X M (2020). Isoprene mixing ratios measured at twenty sites in China during 2012–2014: comparison with model simulation. Journal of Geophysical Research: Atmospheres, 125(24): e2020JD033523

Zhang Y N, Zhang Z S, Chan C Y, Engling G, Sang X F, Shi S, Wang X M (2012). Levoglucosan and carbonaceous species in the background aerosol of coastal Southeast China: case study on transport of biomass burning smoke from the Philippines. Environmental Science and Pollution Research, 19(1): 244–255

Zhao B, Wang S X, Hao J M (2024). Challenges and perspectives of air pollution control in China. Frontiers of Environmental Science & Engineering, 18(6): 68

Zhou J M, Ho S S H, Cao J J, Zhao Z Z, Zhao S Y, Zhu C S, Wang Q Y, Liu S X, Zhang T, Zhao Y Z, et al. (2018). Chemical characterization of $PM_{2.5}$ from a southern coastal city of China: applications of modeling and chemical tracers in demonstration of regional transport. Environmental Science and Pollution Research, 25(21): 20591–20605

Zhu T, Liu Y J, Xu S Q, Dong G H, Huang C R, Sang N, Zhang Y H, Su G Y, Chen J W, Gong J C, et al. (2024). Advances and perspectives in environmental health research in China. Frontiers of Environmental Science & Engineering, 18(6): 76